International Journal of Hydrogen Energy 97 (2025) 649–656

Contents lists available at ScienceDirect

International Journal of Hydrogen Energy

journal homepage: www.elsevier.com/locate/he

# Increasing the efficiency of a conversion gas turbine engine by adding hydrogen to fuel gas☆

G.E. Marin *, A.V. Titov, A.R. Akhmetshin, A.V. Ishalin

*Kazan State Power Engineering University, Department of Power Engineering, Krasnoselskaya St., 51, Kazan, 420066, Russian Federation*

ARTICLE INFO

*Keywords:*
Hydrogen
Hydrogen technologies
Decarbonization

ABSTRACT

Hydrogen, as a zero-carbon fuel, is becoming an important component for decarbonizing the economy. It can be used not only as a storage medium, but also as a fuel for power generation equipment. Hydrogen is very different in its energy properties (high calorific value, high combustion rate), which are very different from traditional gas turbine fuels, so when burning hydrogen, new unexplored problems may arise during the operation of main and auxiliary equipment.

To introduce hydrogen technologies into the traditional energy system, new approaches to equipment operation are required. Gas turbines, unlike other power equipment, can be configured to burn any gaseous fuel that meets the requirements for the combustion chamber. Combustion of 100% $H_2$ in the combustion chamber of an operating gas turbine is impossible without deep modernization; this can cause damage to the main and auxiliary equipment. Gas turbines powered by hydrogen will be an important component in the decarbonization of all industries.

The article discusses the variable operating modes of a gas turbine unit with a capacity of 18 MW, depending on the percentage of $H_2$ in natural gas. The traditional fuel for gas turbines is natural gas; the presented study considers adding up to 20% hydrogen to the original natural gas. The addition of hydrogen fuel affects the operating mode of the turbine. The operation of a gas turbine unit at various outside temperatures, operation at full and partial load in the conditions of the wholesale electricity market is considered.

NOMENCLATURE

| | |
|---|---|
| Abroveatura | |
| Letters of the Latin alphabet | |
| *CCS* | Carbon capture and storage |
| $G_{in}$ | Engine inlet flow |
| $G_{out}$ | Engine outlet flow |
| $\frac{\Delta\overline{T}}{\theta}$ | Relative value of the complex parameter used to determine the heat recovery coefficient |
| $\overline{C}_\tau$ | Relative value of the heat capacity of the coolant |
| $\overline{\sigma}$ | Relative value of total pressure recovery coefficient |
| $\overline{x}$ | Relative argument value |
| $\overline{C}_\tau$ | Relative value of the heat capacity of the coolant, liquid phase |
| $\Delta T$ | Temperature difference |
| $\theta$ | Complex value |
| $T_2^*$ | Temperature of gas stagnation in the chamber outlet section |
| $T_1^*$ | Temperature of gas stagnation in the inlet section of the chamber |

(continued on next column)

(*continued*)

| | |
|---|---|
| $T_{\delta 1}$ | Coolant inlet temperature |
| $T_{\delta 2}$ | Coolant outlet temperature |
| $G_{nm1}$ | Reduced air flow |
| $G_1$ | Air (gas) flow at the inlet |
| $P_1^*$ | Inlet air (gas) stagnation pressure |
| $R$ | Gas constant of air (gas) |
| $\lambda_1$ | Reduced speed |
| $C_{ss1}$ | Superficial speed |
| $M_1$ | Mach number |
| $C$ | Sound speed |
| $R$ | Universal gas constant |
| $T_1$ | Flow temperature |
| $k$ | Adiabatic exponent |
| $q(\lambda_1)$ | Gas dynamic function |
| $k$ | Boltzmann's constant |
| $H_{vg}^*$ | Enthalpy at a given air temperature |

(continued on next page)

☆ This paper is the English version of the paper reviewed and published in Russian in "*International Scientific Journal for Alternative Energy and Ecology*" ISJAEE, 2024, Issue (429), #12.

* Corresponding author.
*E-mail address:* george64199@mail.ru (G.E. Marin).

https://doi.org/10.1016/j.ijhydene.2024.11.304
Received 29 September 2024; Accepted 16 November 2024

(*continued*)

| | |
|---|---|
| $T_g^*$ | Gas temperature |
| $q_F$ | Fuel gas consumption |
| $H_{CP}^*$ | Enthalpies of combustion products during complete combustion of fuel |
| $\alpha$ | Excess air ratio |
| $H_{er}^*$ | Lower calorific value at the end point |
| $H_1^*$ | Lower heating value at starting point |
| $Hu$ | Lower heating value of fuel (mixture) |
| $\eta'$ | Thermal efficiency of the flow mixture |
| $H_0$ | Net calorific value, average value for fuel mixture |
| $n_1$, $n_2$, $n_3$, $n_4$ | Shaft rotation speed |
| $\rho$ | Density of methane-hydrogen mixture |
| $\omega_i$ | Mass fraction of the i-th component |
| $H_{uMH}$, | Lower calorific value of methane-hydrogen mixture |
| $H_{ui}$ | Lower calorific value of the i-th component |
| $L_0$ | Stoichiometric coefficient of methane-hydrogen mixture |
| $m_0$ | Mass of air required for complete combustion |
| $m_{0i}$ | Mass of oxygen reacting stoichiometrically with the i-th component |
| $W_n$ | Wobbe index |
| $H_u$ | Lower calorific value |
| $\rho_g$ | Gas density |
| $\rho_{air}$ | Air density |
| $T_{amb\ t}$ | Ambient temperature |
| $P_{amb\ pr}$ | Ambient air pressure |
| $\phi$ | Importance |
| $N$ | Gas turbine power |
| $H_2$ | Hydrogen |
| $CO_2$ | Carbon dioxide |
| $C_3H_8$ | Propane |
| $CH_4$ | Methane |
| $C_4H_{10}$ | n-butane |
| $C_4H_{10}$ | i-butane |
| $C_2H_6$ | Ethane |
| MW | Power |
| $m^3/h$ | Fuel gas consumption |
| K | Kelvin |
| °C | Degree Celsius |
| rpm | Rotation frequency |
| MJ/kg | Calorific value |
| $kg/m^3$ | Density |
| $MJ/m^3$ | Calorific value |
| kPa | Pressure |
| % | Procent |
| Letters of the Russian alphabet | |
| GTU | Gas turbine unit |
| RES | Renewable energy |
| NPP | Nuclear power plant |
| GTE | Gas turbine engine |
| E | Efficiency |
| ID | Input device |
| LPC | Low pressure compressor |
| HPC | High pressure compressor |
| CC | Combustion chamber |
| HPT | High pressure turbine |
| LPT | Low pressure turbine |
| PT | Power turbine |
| EG | Electric generator |
| $ID_{out}$ | Output device |
| AS GRET | Automated system for gas-dynamic calculations of power turbomachines |
| A | Air |
| $T_{in}$ | Inlet temperature |
| $T_{out}$ | Outlet temperature |
| MPC | Medium pressure compressor |
| MPT | Medium pressure turbine |
| WHB | Waste heat boiler |
| C | Chimney |
| NG | Natural gas |

## 1. Introduction

Population growth and technology development are constantly increasing the need for energy use. According to forecasts of international energy unions, natural gas and oil are the final product, and the use of hydrocarbon fuels has a negative impact on the environment [1–3]. A number of scientists express the opinion that the combustion of hydrocarbons leads to the destruction of the Earth's ozone layer, so it is important to find an alternative to traditional fuels [4,5]. An important component when using alternative fuels is minimizing emissions. Hydrogen may be a promising fuel, but the methods for its production are different. Table 1 shows the most common types of hydrogen fuel production.

The main production of hydrogen occurs using methane conversion technology [6]. In Fig. 1 shows the share distribution of hydrogen production.

As can be seen from Fig. 1 Most of the hydrogen produced is accompanied by $CO_2$ emissions during its production.

This study examines the issue of burning hydrogen fuel in the combustion chamber of a gas turbine unit. Converting gas turbines to combustion of hydrogen fuel is a promising direction, allowing to partially reduce emissions from existing power equipment [7]. Almost all manufacturers of power equipment are implementing the transition to hydrogen fuel, but long-term operation on 100% $H_2$ is currently not implemented in gas turbine plants. Firstly, this is the high cost of hydrogen, and secondly, this is expensive auxiliary equipment.

The use of hydrogen in the energy sector to reduce emissions to zero is only possible if the hydrogen fuel is produced with minimal $CO_2$ emissions. When designing and operating auxiliary equipment, the following problems arise.

1. Embrittlement of metals of main and auxiliary equipment [8,9].
2. Development of new low-emission combustion chambers that allow the combustion of hydrogen fuel in any percentage [10,11].
3. Introduction of new expensive structural materials into the gas turbine cycle [12,13].

## 2. Mathematical model of a gas turbine engine

Solving the problems presented above is possible only by designing new gas turbines with high energy and environmental characteristics; operating turbines can burn a mixture of natural gas and hydrogen fuel [14–17].

A conversion three-shaft gas turbine engine (GTE) with a power of 18 MW was selected as the object under study. The main characteristics of the gas turbine engine are presented in Table 2.

Fig. 2 shows the functional diagram of the GTE.

In Fig. 2 the following designations are accepted: ID – input device; LPC – low pressure compressor; HPC – high pressure compressor; CC – combustion chamber; HPT – high pressure turbine; LPT – low pressure turbine; ST – power turbine; E – electric generator; $ID_{Out}$ – output device; $G_{in}$ – flow rate at the engine inlet; $G_{out}$ – flow rate at the engine outlet.

### 2.1. Combustion chamber characteristics

Due to the fact that the addition of hydrogen fuel occurs in the combustion chamber, with the design remaining unchanged, it is necessary to model the gas turbine unit in all load ranges. To study the characteristics, a mathematical model was created in the «AS GRET » software package (Automated system for gas-dynamic calculations of power turbomachines) [18]. This software package allows you to model nodes using a block diagram. The addition of hydrogen to the gas turbine cycle required changes to the calculation algorithm. The modified calculation algorithm is presented below. The calculation of the main combustion chamber is based on the use of its characteristics, which are specified in the form of dependences of the total pressure recovery coefficient and the fuel combustion efficiency coefficient on various parameters used as arguments of the dependencies.

The following dependencies are used as characteristics of the combustion chamber:

**Table 1**
Types of hydrogen fuel production.

| Classification of hydrogen by color | Receiving technology | Carbon footprint of hydrogen fuel |
|---|---|---|
| Green | Electrolysis of water using electricity, obtained from RES | 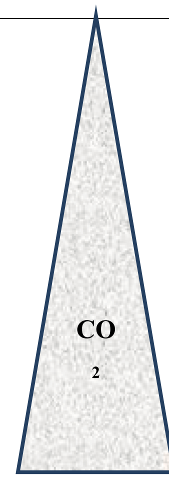 |
| Orange | Electrolysis of water using electricity from mixed production (RES, NPP, GTP) | |
| Yellow | Electrolysis of water using electricity, received at the NPP | |
| Turquoise | Methane pyrolysis | |
| Blue | Steam methane reforming + CCS | |
| Brown | Coal gasification | |
| Grey | Steam reforming of methane | |

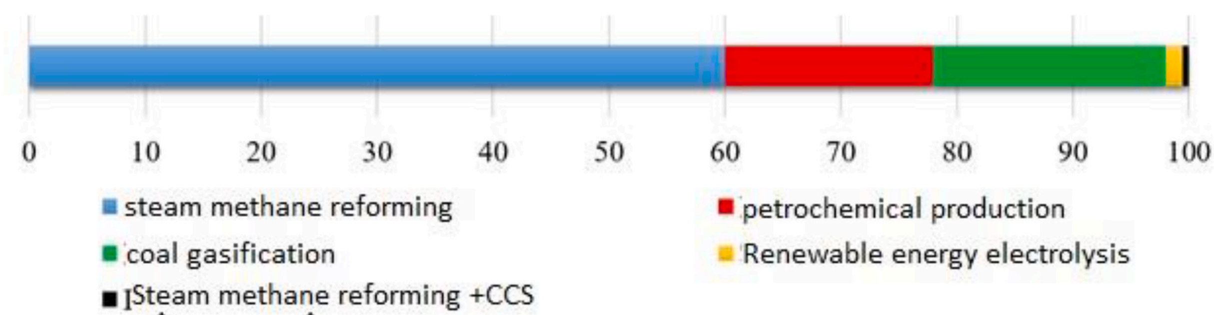


**Fig. 1.** Share distribution of hydrogen production.

**Table 2**
Main parameters of the GTE.

| Parameter name | Meaning |
|---|---|
| Power, MW | 18 |
| Effective efficiency, % | 31 |
| Pressure increase rate | 9 |
| Fuel gas consumption, $m^3/h$ | 6500 |
| Gas temperature in front of the turbine, K | 1188 |
| Gas temperature at the outlet of a free turbine, °C | 427 |
| Range of rotation speed of the free turbine drive shaft, rpm | 3975–5565 |

$$\left(\frac{\Delta \overline{T}}{\theta}\right) = f(\overline{x}), \overline{C}_m = f(\overline{x}), \overline{\sigma} = f(\overline{x}),$$

where: $\frac{\Delta \overline{T}}{\theta}$– relative value of the complex parameter used to determine the heat recovery coefficient;

$\overline{C}_\tau$ – relative value of the heat capacity of the coolant;

$\overline{\sigma}$ –relative value of the total pressure recovery coefficient;

$\overline{x}$ – relative value of the argument, which can be any parameter from the array « A», the value of which is determined at the time of use.

The relative value is determined through simple transformations:

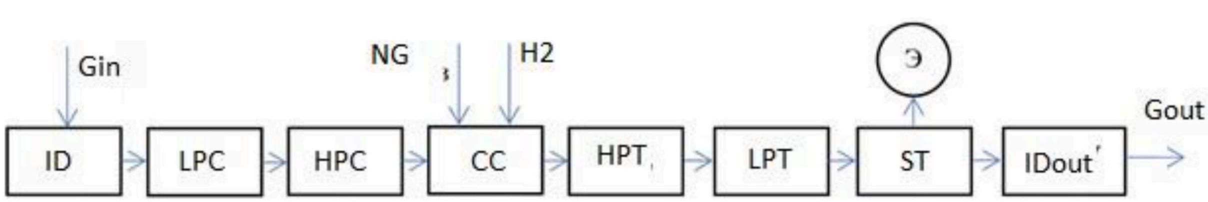


**Fig. 2.** Functional diagram of a three-shaft GTE.

$$\left(\frac{\Delta\overline{T}}{\theta}\right)=\frac{\left(\frac{\Delta T}{\theta}\right)}{\left(\frac{\Delta T}{\theta}\right)_H},\overline{C}_{m6}=\frac{C\rho l}{C\rho l_H},\overline{\sigma}=\frac{\sigma}{\sigma_H},\overline{\overline{x}}=\frac{x}{x_H},$$

where $\overline{C}pl$ - relative value of the heat capacity of the coolant, liquid phase.

The index « H » corresponds to the design operating mode. The value of the complex parameter is determined by the following formulas:

$$\Delta T=T_2^*-T_1^*,$$

$$\theta=\frac{(T_1-T_2^*)-(T_2-T_1^*)}{\ln\left(\frac{T_1-T_2^*}{T_1-T_1^*}\right)},$$

where:$\Delta T$ – temperature difference;

$\theta$– complex meaning;

$T_2^*$ and $T_1^*$– gas stagnation temperature in the outlet and inlet sections of the chamber;

$T_1$ and $T_2$ – coolant temperature at the inlet and outlet.

The value of the reduced air flow ($G_{nm1}$) is calculated, which can be used as an argument for the dependence σ = f(x):

$$G_{\pi r1}=\frac{G_1\sqrt{T_1^*}}{P_1^*},$$

where $G_1$–air (gas) flow at the inlet;

$P_1^*$ – stagnation pressure of air (gas) at the inlet.

The value of the gas constant of air (gas) $R=f(q_{T1})$ is calculated.

The reduced speed can be found as follows ($\lambda_1$):

$$\lambda_1=C_1/\ Css_1,$$

where $Css_1$ – superficial speed.

Mach number ($M_1$) is calculated:

$$M_1=\frac{C}{\sqrt{1000{\cdot}R{\cdot}k{\cdot}T_1}},$$

where $C$-sound speed;

$R$ – universal gas constant;

$T_1$ – flow temperature, K.

The gas dynamic function $q(\lambda_1)$ is calculated:

$$q(\lambda_1)=\left(\frac{k+1}{2}\right)^{\frac{1}{k-1}}\cdot\lambda_1\left(1-\frac{k-1}{k+1}\lambda_1^2\right)^{\frac{1}{k-1}},$$

where $k$ – Boltzmann's constant.

Checks to see if the combustion chamber is working. If $T_1^*<T_A^*$, then the enthalpy values are calculated at a given air temperature($H_{vg}^*$):

$$H_{vg}^*=f\left(T_r^*,q_T=0\right),$$

where $T_g^*$ – gas temperature;

$q_F$ – fuel gas consumption.

Enthalpy of combustion products with complete combustion of fuel and at the same temperature ($H_{cp}^*$):

$$H_{cp}^*=f\left(T_r^*,q_{T,\alpha=1}\right),$$

where $\alpha$– excess air ratio.

Then the relative fuel consumption value is calculated:

$$q_F=\frac{H_{er}^*-H_1^*}{Hu{\cdot}\eta'-H_{CP}^*+H_0}$$

where $H_{er}^*$– lower calorific value at the end point;

$H_1^*$ – lower calorific value at the starting point;

$Hu$– lower heating value of fuel (mixture);

$\eta'$– thermal efficiency of the flow mixture;

$H_0$ – lower calorific value, average value for a fuel mixture.

Excess air ratio:

$$\alpha=\frac{1}{q_F{\cdot}L_0}$$

In Fig. 3 shows the design node diagram of the GTU.

In Fig. 3 the following designations are used: A – air; $T_{in}$ – inlet temperature; $T_{out}$ – outlet temperature; 1 – low pressure compressor; 2 – medium pressure compressor; 3 – high pressure compressor; 4 – high pressure turbine; 5 – medium pressure turbine; 6 low pressure turbine; 7 – power turbine; 8 – waste heat boiler; 9 – chimney; 10 – combustion chamber; $n_1$, $n_2$, $n_3$, $n_4$ – shaft rotation speeds.

## 3. Adding hydrogen to natural gas

Natural gas containing 98.6% methane by volume was selected as the source fuel. The addition of hydrogen fuel to the fuel composition must be carried out based on maximum energy efficiency and minimal design changes [19–21]. To preserve the design of the gas turbine unit, the addition of hydrogen should not exceed 20%. To determine the optimal composition, we will calculate fuel with a range of hydrogen admixture from 10% to 20% by volume in increments of 2%. The composition of the original fuel is presented in Table 3.

Table 4 presents the main characteristics of the mixture of natural gas and hydrogen fuel.

To determine the most suitable fuel, its lower heating value will be calculated. Fuel calculations will be made based on Table 4.

The sum of the masses of the components contained in 1 $m^3$ of methane-hydrogen mixture will be the mass of 1 $m^3$ of methane-hydrogen mixture, taking into account the densities of each component, i.e. its density will correspond to:

$$\rho=\sum\nolimits_i\rho_i,$$

where $\rho$ – density of methane-hydrogen mixture, kg/$m^3$.

We determine the mass fraction of each component:

$$\omega_i=\frac{\rho_i}{\rho},$$

where $\omega_i$ – mass fraction of the i-th component.

The results of calculating the mass fractions of components are given in Table 4.

Knowing the mass fractions of the components, the mass calorific value is calculated. For the composition under consideration, the lower calorific value of the methane-hydrogen mixture ($H_{uMH}$, MJ/kg) is:

$$H_{uMB}=\sum\omega_iH_{ui},$$

where $H_{ui}$ – lower calorific value of the i-th component, MJ/kg.

Knowing the density and percentage of components, the volumetric calorific value is calculated. For the composition under consideration, the lower calorific value of the methane-hydrogen mixture ($H_{uMH}$, MJ/$m^3$) is:

$$H_{uMH}=\sum\rho_iH_{ui},$$

The stoichiometric coefficient of the methane-hydrogen mixture $L_0$, kg air/kg fuel is the mass of air required for complete combustion of 1 kg of methane-hydrogen mixture. To do this, it is necessary to estimate the amount of oxygen that is required for the combustion of all flammable components of the methane-hydrogen mixture, i.e. hydrogen $H_2$, methane $CH_4$, ethane $C_2H_6$, $C_3H_8$ propane and $C_4H_{10}$ butane (Table 5).

The mass of air required for complete combustion can be determined

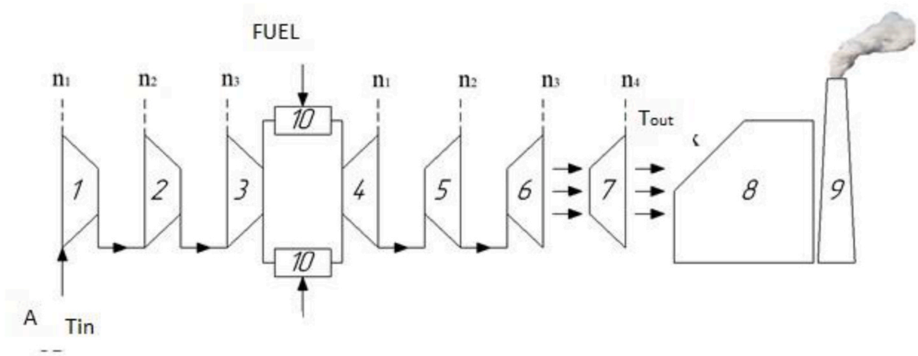


**Fig. 3.** Design node diagram of the GTU.

**Table 3**
Composition of the original fuel.

| Element | Formula | Percentage Composition |
|---|---|---|
| Methane | $CH_4$ | 98,6% |
| Propane | $C_3H_8$ | 0,3% |
| n-butane | $C_4H_{10}$ | 0,15% |
| i-butane | $C_4H_{10}$ | 0,05% |
| Ethane | $C_2H_6$ | 1% |

by the following formula:

$$m_0 = \sum_i \omega_i m_{0i}$$

where $m_{0i}$ is the mass of oxygen that reacts stoichiometrically with the i-th component, kg. Considering that 1 kg of air contains 0.232 kg of oxygen, we obtain the stoichiometric coefficient shown in Fig. 4.

The amount of air required for the combustion of 1 $m^3$ of fuel, and the stoichiometric coefficient:

$$L_0 = \frac{m_0}{0,232}$$

The energy properties of natural gas mixed with hydrogen fuel are presented in Table 6.

### 3.1. *Wobbe index*

The Wobbe index is a characteristic that allows us to understand the interchangeability of fuel gases in a gas turbine installation. Changing the fuel composition leads to a change in this index; the range of changes in values should be ±5%. This allows you to make minimal changes to the combustion mode, changes in emissions from the GTU and to fuel consumption. A deviation of more than 5% of the Wobbe index entails the transition of equipment into unstable operating modes [22–26].

The Wobbe index ($W_n$) is calculated as follows:

$$W_n = \frac{H_u}{\sqrt{\frac{\rho_r}{\rho_g}}}$$

where $H_u$ – lower calorific value;

$\rho_g$ – gas density;

$\rho_{air}$ –air density.

The calculation results are presented in Fig. 5.

In fuel with an additive of 20% by volume, all conditions for stable operation of a gas turbine are maintained with minimal design changes and an optimal operating range. All subsequent calculations will be made with the mixtures presented in Table 6.

### 3.2. *Change in the main energy characteristics of the turbine*

The initial data for the study were taken as $T_{amb\ t} = 288.15$ K, $P_{amb\ pr} = 101.3$ kPa, $\phi = 60$ %. The design power of the gas turbine is $N = 18$ MW, the temperature after the combustion chamber is 1188 K. During

**Table 5**
Oxidizer consumption per 1 kg (1 $m^3$) of combustible gas.

| Oxidizer | $H_2$ | $CH_4$ | $C_2H_6$ | $C_3H_8$ | $C_4H_{10}$ |
|---|---|---|---|---|---|
| Oxygen(kg) | 7,9 | 3,99 | 3,73 | 3636 | 3586 |

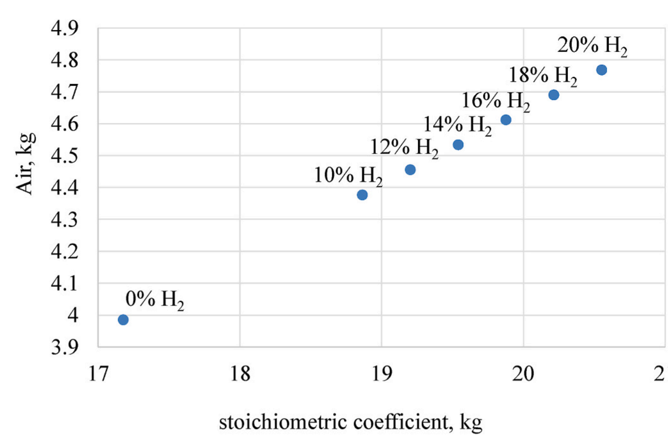


**Fig. 4.** The amount of air required for the combustion of 1 $m^3$ of fuel, and the stoichiometric coefficient.

**Table 4**
Gas composition when adding hydrogen to the original fuel.

| Element | NG | NG+10% hydrogen | NG+12% hydrogen | NG +14% hydrogen | NG +16% hydrogen | NG +18% hydrogen | NG +20% hydrogen |
|---|---|---|---|---|---|---|---|
| Methane | 0,985 | 0,8865 | 0,8668 | 0,8471 | 0,8274 | 0,8077 | 0,788 |
| Propane | 0,003 | 0,0027 | 0,00264 | 0,00258 | 0,00252 | 0,00246 | 0,0024 |
| Butane | 0,0015 | 0,00135 | 0,00132 | 0,00129 | 0,00126 | 0,00123 | 0,0012 |
| Isobutane | 0,0005 | 0,00045 | 0,00044 | 0,00043 | 0,00042 | 0,00041 | 0,0004 |
| Ethane | 0,01 | 0,009 | 0,0088 | 0,0086 | 0,0084 | 0,0082 | 0,008 |
| hydrogen | 0 | 0,1 | 0,12 | 0,14 | 0,16 | 0,18 | 0,2 |

**Table 6**
Energy properties of natural gas mixed with hydrogen fuel.

| Name | Hydrogen content, % | | | | | | |
|---|---|---|---|---|---|---|---|
| | 0% | 10% | 12% | 14% | 16% | 18% | 20% |
| Density, kg/m$^3$ | 0,731 | 0,66 | 0,654 | 0,641 | 0,628 | 0,615 | 0,602 |
| Heat of combustion, MJ/m$^3$ | 36,5 | 34,05 | 33,56 | 33,07 | 32,58 | 32,09 | 31,6 |
| Molar mass of fuel, g/mol | 16,34 | 14,9 | 14,62 | 14,34 | 14,05 | 13,76 | 13,48 |
| Lower calorific value, MJ/kg | 49,89 | 50,8 | 51,04 | 51,26 | 51,49 | 51,73 | 51,98 |

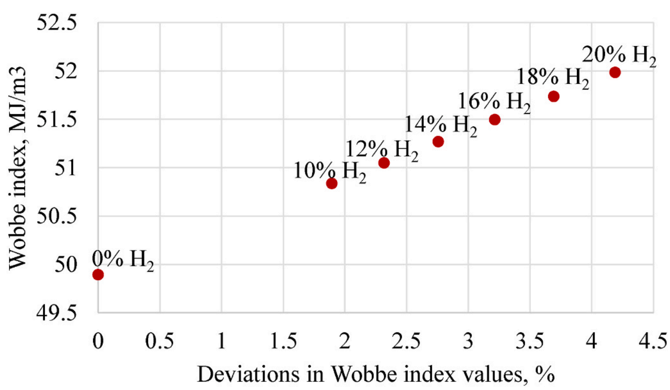


**Fig. 5.** Wobbe index indicators.

the study, the following modes will be considered: external and internal throttle characteristics, as well as climatic characteristics. The parameters defining the mode, in the first case, is the power consumed by the drive units and is calculated from 15 MW to 19 MW, in the second case, the temperature of the gases after the combustion chamber, it is taken from 1148 K to 1198 K. The climatic characteristic is calculated at a constant power of 18 MW and outside air temperature in the range from 253 K to 303 K.

Based on the results of the study, the main characteristics of the engine when operating on natural gas with the addition of hydrogen were obtained, presented in Fig. 6.

After an increase in the outside air temperature, the efficiency of the installation decreases (Fig. 6), however, with the addition of hydrogen, the efficiency can increase slightly.

The change in fuel consumption relative to natural gas without adding hydrogen with a change in outside air temperature is shown in Fig. 7.

Fig. 7 shows the change in fuel gas consumption when adding hydrogen fuel; an increase in the amount of hydrogen in the mixture with natural gas leads to a decrease in overall fuel consumption.

The fuel consumption of various types of fuel with changes in outside air temperature is shown in Fig. 8.

By adding hydrogen, fuel consumption is significantly reduced (Fig. 8). Savings of initial fuel occur from 3.15% to 3.5% at 10% hydrogen by volume, from 7.7% to 7.9% at 20% hydrogen or a maximum of 375 kg/h of initial fuel at a temperature of 253–303 K. The dependence is linear (Fig. 8). When the outside air temperature changes, the temperature at the outlet of the units changes by an equal value at most of the temperatures under consideration.

The air consumption at the engine inlet of various types of fuel with a change in outside air temperature is shown in Fig. 9.

When varying power from 15 MW to 19 MW, the temperature change occurs curvilinearly with a gradual increase in the gap between different types of fuel. For 10% hydrogen it changes from 0.017% to 0.026%, for 20% hydrogen from 0.036% to 0.055%. As the power increases from 15 MW to 19 MW, the combustion chamber temperature increases curvilinearly with a gradual increase in the gap between different types of fuel. For 10% hydrogen it changes from 0.03% to 0.04%, for 20% hydrogen from 0.07% to 0.09%.

The change in efficiency relative to natural gas without adding hydrogen with a change in the power of the units is illustrated in Fig. 10.

When the power increases from 15 MW to 19 MW, the maximum increase in efficiency occurs by 16 MW and reaches a maximum increase of 4% (Fig. 10). After this, there is a slight decrease in the increase in efficiency.

Fuel consumption of various types with changes in unit power is shown in Fig. 11.

By adding hydrogen, fuel consumption is significantly reduced. Savings in initial fuel occur from 3.2% to 3.7% at 10% hydrogen by volume, from 7.8% to 8% at 20% hydrogen or a maximum of 380 kg/h of initial fuel at a power of 15–19 MW (Fig. 11).

Maneuvering the operating mode of the equipment demonstrates the best performance of fuel with the addition of hydrogen at any power. The results obtained using the throttle characteristic are similar to the climatic ones, with a slight increase in efficiency, temperatures in the combustion chamber and the cut-off from the output device. Hourly fuel consumption shows the same high figures, from 3.2% to 8% savings on the original fuel.

As the temperature of the combustion chamber varies, the outlet temperature increases in a straight line with a gradual increase in the gap between different types of fuel. For 10% hydrogen it changes from 0.012% to 0.015%, for 20% hydrogen from 0.022% to 0.03%.

The change in fuel consumption relative to natural gas without adding hydrogen with a change in temperature in the combustion chamber is shown in Fig. 12.

The temperature of the combustion chamber changes from 1148 K to 1198 K; temperature control allows you to obtain higher values. Hourly fuel consumption allows saving from 3.25% at 1148 K to 8.10% at 1198

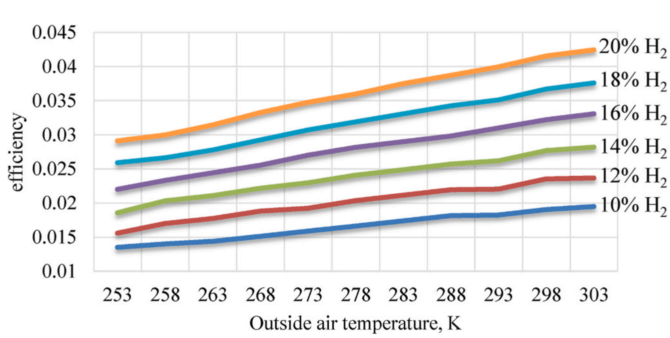


**Fig. 6.** Changing the efficiency of the installation with the addition of hydrogen and changing the outside air temperature.

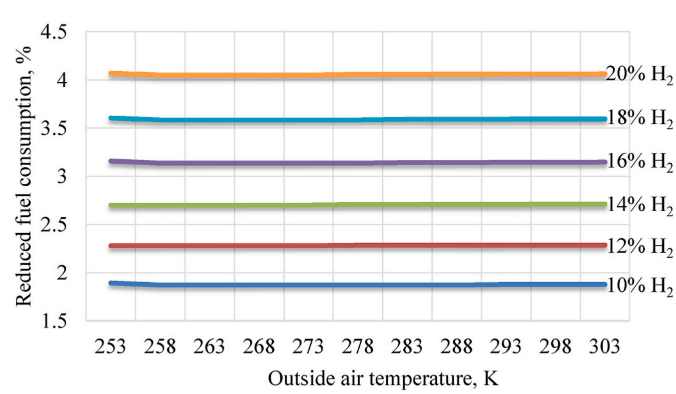


**Fig. 7.** Change in fuel consumption relative to natural gas without adding hydrogen with a change in outside air temperature.

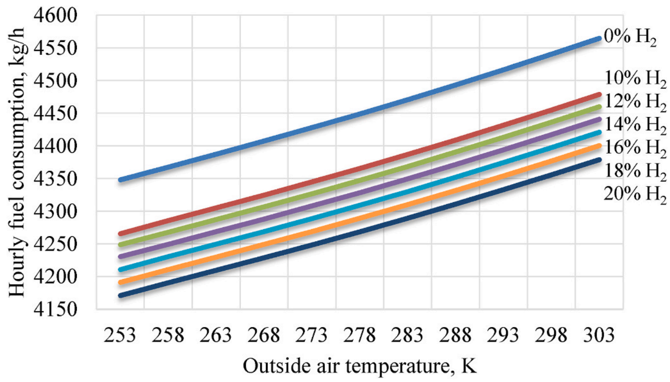


**Fig. 8.** Fuel consumption of various types of fuel with changes in outside air temperature.

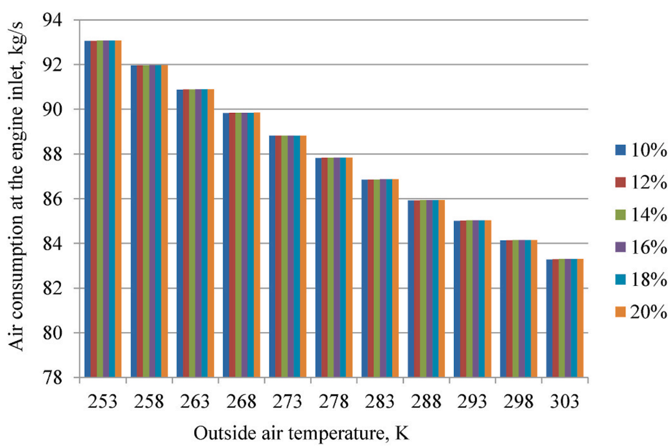


**Fig. 9.** Air consumption at the engine inlet of various types of fuel with changes in outside air temperature.

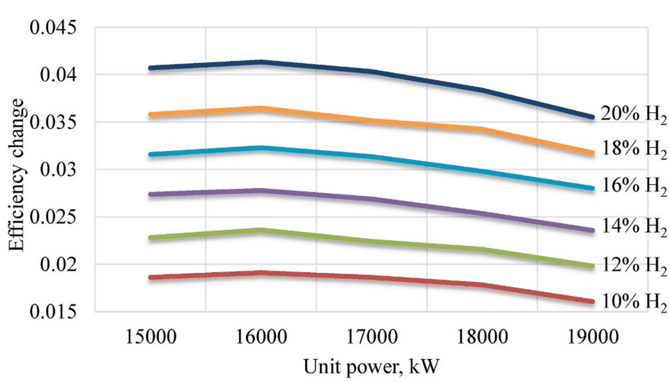


**Fig. 10.** Change in efficiency relative to natural gas without adding hydrogen with a change in the power of the units.

K of the original fuel (Fig. 12). Other indicators show less difference compared to climatic characteristics.

## 4. Conclusions

A gas turbine unit with a developed combustion system to operate on natural gas is being investigated. Fuel efficiency, while reducing emissions, is an important component when operating power equipment. A mixture of fuel gas is considered; hydrogen fuel is added to the original natural gas in the range from 10 to 20%, while the share of natural gas is reduced from 100 to 80% at the same time. The addition of hydrogen

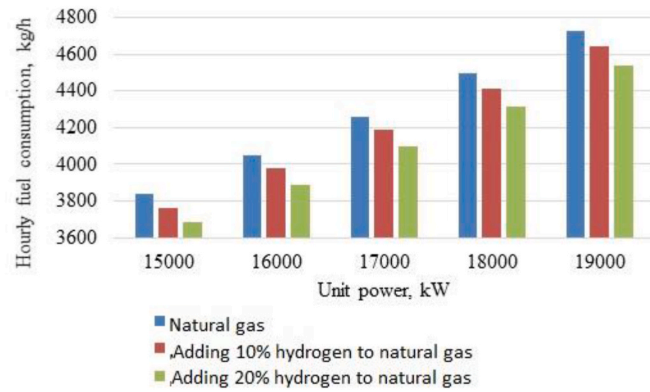


**Fig. 11.** Fuel consumption of various types with changes in unit power.

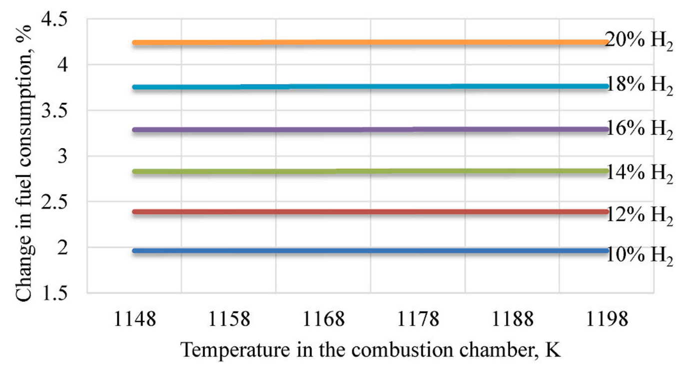


**Fig. 12.** Change in fuel consumption relative to natural gas without adding hydrogen with a change in temperature in the combustion chamber.

results in a 3.5% reduction in fuel consumption when adding 10% hydrogen, and when adding 20% the reduction in fuel consumption reaches 7.9%. It is important to note that when hydrogen fuel is added, the temperature in the gas turbine combustion chamber increases by 0.08%, which indicates that the combustion chamber cooling system is operating within the acceptable range. When hydrogen is added, the effective efficiency increases; the highest value is achieved at a power of 16 MW.

Despite the high energy characteristics of the gas turbine, it is worth noting that adding more than 20% hydrogen is possible only after a thorough modernization of the gas turbine unit and fuel treatment system.

## References


[1] Kivimaa P, Sivonen MH. How will renewables expansion and hydrocarbon decline impact security? Analysis from a socio-technical transitions perspective. Environ Innov Soc Transit 2023;48:100744.

[2] Abd AA, Naji SZ, Hashim AS. Effects of non-hydrocarbons impurities on the typical natural gas mixture flows through a pipeline. J Nat Gas Sci Eng 2020;76:103218.

[3] Gałko G, Mazur I, Rejdak M, Jagustyn B, Hrabak J, Ouadi M, Jahangiri H, Sajdak M. Evaluation of alternative refuse-derived fuel use as a valuable resource in various valorised applications. Energy 2023;263(Part D):125920.

[4] Gao D, Li Z, Liu P, Zhao J, Zhang Y, Li C. Coordinated energy security model taking strategic petroleum reserve and alternative fuels into consideration. Energy 2018; 145:171–81.

[5] Marin G, Osipov B, Mendeleev D. Study of the properties of fuel gas in gas turbine plants depending on its composition. Lect Notes Mechan Eng 2022:403–12.

[6] Zakaria Z, Kamarudin SK. Direct conversion technologies of methane to methanol: an overview. Renew Sustain Energy Rev 2016;65:250–61.

[7] Marin GE, Osipov BM, Titov AV, Akhmetshin AR. Simulation of the operation of a gas turbine installation of a thermal power plant with a hydrogen. Fuel Prod Syst Int J Hydrogen Energy 2023;48(12):4543–50.

[8] Zamanzade M, Barnoush A. An overview of the hydrogen embrittlement of iron aluminides. Proc Mater Sci 2014;3:2016–23.

[9] Honma Y, Kayano R. Study of embrittlement of the 2.25Cr-1Mo-V steel weld metal by hydrogen charge and high pressure hydrogen gas environment. Procedia Eng 2015;130:571–82.
[10] Gicquel LYM, Staffelbach G, Poinsot Large T. Eddy Simulations of gaseous flames in gas turbine combustion chambers. Energy Combust Sci 2012;38(6):782–817.
[11] Al-attab KA, Zainal ZA. Design and performance of a pressurized cyclone combustor (PCC) for high and low heating value gas combustion. Appl Energy 2011;88(4):1084–95.
[12] ÁlvarezTejedor T. 9 - gas turbine materials selection, life management and performance improvement. In: Woodhead publishing series in energy power plant life management and performance improvement. Woodhead Publishing; 2011. p. 330–419.
[13] Adamou A, Turner J, Costall A, Jones A, Copeland C. Design, simulation, and validation of additively manufactured high-temperature combustion chambers for micro gas turbines. Energy Convers Manag 2021;248:114805.
[14] Marin G, Osipov B, Titov A, Akhmetshin A, Shubina A, Novoselova M. Improving the performance of power plants with gas turbine units proceedings - 2022 4th international conference on control systems, mathematical modeling. Automat Energy Eff 2022:832–6. SUMMA 2022.
[15] Marin G, Osipov B, Akhmetshin A. Analysis of the operation of a gas turbine plant when burning hydrogen fuel proceedings. In: 2022 international Russian automation conference, RusAutoCon; 2022. p. 961–5.
[16] SamithaWeerakoon AH, Assadi Trends M. Advances in micro gas turbine technology for sustainable energy solutions: a detailed review. Energy Convers Manag X 2023:100483.
[17] Enagi II, Al-attab KA, Zainal ZA. Combustion chamber design and performance for micro gas turbine application. Fuel Process Technol 2017;166:258–68.
[18] Osipov BM, Titov AV, Khammatov AR. Investigation of power gas turbine drives on the basis of mathematical models. Russ Aeronaut 2010;53:69–72.
[19] Ishaq H, Dincer I. Performance investigation of adding clean hydrogen to natural gas for better sustainability. J Nat Gas Sci Eng 2020;78. Article Number 103236.
[20] Sorgulu F, Ozturk M, Javani N, Dincer I. Experimental investigation for combustion performance of hydrogen and natural gas fuel blends. Int J Hydrogen Energy 2023;48(88):34476–85.
[21] Guo Q, Liu J, Liang W, Wang H. On the explosion characteristics of natural gas with hydrogen and inert gas additions. Process Saf Environ Protect 2023;179:700–13.
[22] Slim BK, Darmeveil HD, Gersen S, Levinsky HB. The combustion behaviour of forced-draught industrial burners when fired within the EASEE-gas range of Wobbe. Index J Nat Gas Sci Eng 2011;3(Iss. 5):642–5.
[23] Worasaen A, Pannucharoenwong N, Benjapiyaporn C, Jongpluempiti J, Vengsungnle P. Suitable study of CBG fuel by considering in Wobbe index from compressed bio-methane gas plant. KhonKaen Univ Thailand Energy Proc 2017;138:278–81.
[24] Roy PS, Ryu C, Park CS. Predicting Wobbe Index and methane number of a renewable natural gas by the measurement of simple physical properties. Fuel 2018;224:121–7.
[25] Zachariah-Wolff JL, Egyedi TM, Hemmes K. From natural gas to hydrogen via the Wobbe index: the role of standardized gateways in sustainable infrastructure transitions Journal of Hydrogen Energy 2007;32(9):1235–45.
[26] Mendeleev DI, Maryin GE, Akhmetshin AR. Improving the efficiency of combined-cycle plant by cooling incoming air using absorption refrigerating machine. IOP Conf Ser Mater Sci Eng 2019;643:012099.